



EUROfusion

WPBB-PR(17) 17161

K Mukai et al.

**Effect of moisture in sweep gas on
chemical compatibility between ceramic
breeder and EUROFER97**

Preprint of Paper to be submitted for publication in
Fusion Engineering and Design



This work has been carried out within the framework of the EUROfusion Consortium and has received funding from the Euratom research and training programme 2014-2018 under grant agreement No 633053. The views and opinions expressed herein do not necessarily reflect those of the European Commission.

This document is intended for publication in the open literature. It is made available on the clear understanding that it may not be further circulated and extracts or references may not be published prior to publication of the original when applicable, or without the consent of the Publications Officer, EUROfusion Programme Management Unit, Culham Science Centre, Abingdon, Oxon, OX14 3DB, UK or e-mail Publications.Officer@euro-fusion.org

Enquiries about Copyright and reproduction should be addressed to the Publications Officer, EUROfusion Programme Management Unit, Culham Science Centre, Abingdon, Oxon, OX14 3DB, UK or e-mail Publications.Officer@euro-fusion.org

The contents of this preprint and all other EUROfusion Preprints, Reports and Conference Papers are available to view online free at <http://www.euro-fusionscipub.org>. This site has full search facilities and e-mail alert options. In the JET specific papers the diagrams contained within the PDFs on this site are hyperlinked

Effect of moisture in sweep gas on chemical compatibility between ceramic breeder and EUROFER97

Keisuke Mukai^a, Maria Gonzalez^b, Regina Knitter^a

^a Institute for Applied Materials (IAM), Karlsruhe Institute of Technology, 76021 Karlsruhe, Germany.

^b National Fusion Laboratory, Division of Fusion Technology, CIEMAT, 28040 Madrid, Spain.

Abstract

Effect of moisture in sweep gas on chemical compatibility between ceramic breeder (Li_4SiO_4 with 20 mol% of Li_2TiO_3) and EUROFER97 was examined in this study. These materials were contacted and heated at 623, 823, and 1073 K for up to 12 weeks where the H_2O concentrations of the outlet gas were 4-8 vol.%. In the breeder specimen, Li_4SiO_4 was preferably decomposed into Li_2SiO_3 with a possible formation of Li_2O or LiOH depending on environmental condition. Formation of corrosion layers on the EUROFER specimen was enhanced in the wet condition, especially at the elevated temperatures of 823 and 1073 K. Unlike our previous work in dry sweep gas condition, an extrapolation from data of the elevated temperatures to 623 K was not feasible in the wet atmosphere, which could derive from the difference of the chemical form in the breeder specimen. Effective diffusion coefficient of oxygen into EUROFER at 623 K was given to be $4.5 \times 10^{-13} \text{ cm}^2/\text{s}$ and a possible thickness of the corrosion layer after a 2-year use was predicted.

Introduction

The helium cooled pebble bed (HCPB) blanket concept is being developed toward a future implementation in a DEMO fusion reactor, in which ceramic breeder pebbles are packed to produce tritium by nuclear transmutation of Li.^[1] During years of an operation period, the pebbles are contacted with structural steel of the blanket at an elevated temperature of 623 K, while the temperature of the pebble bed is elevated up to 1173 K.^[2] EUROFER97, a reference structural material for the European DEMO blanket, is a high purity steel composed of Fe, 8.9% Cr, 1.1% W, 0.4% Mn, 0.2% V, 0.1% C, 0.1% Ta, 0.04% Si, and 0.009% Ti to owe high irradiation resistance and low activation capability.^[3] As ceramic breeder material, the ternary oxides of Li_4SiO_4 and Li_2TiO_3 are the most promising candidates owing good chemical stability, low activation property, and fast tritium diffusivity. The mixed composition, Li_4SiO_4 with addition of 10-30 mol% of Li_2TiO_3 , has been proposed as an advanced breeder material to improve mechanical properties of the pebbles.^[4]

In the HCPB concept, inert sweep gas is employed for tritium recovery and transport from the surface of the breeder pebbles. The reference sweep gas is helium with 0.1% addition of H_2 for facilitating tritium release from the ceramic breeder pebbles by taking advantage of hydrogen isotope exchange. Yet, alternative sweep gas composition might improve tritium release. Addition of water vapor to sweep gas, namely $\text{He} + \text{H}_2\text{O}$, can be another option to facilitate tritium release substantially by promoting surface isotope exchange reaction between the gas and tritium on surface of the breeder pebble.^{[5][6]} Furthermore, with a favored release of HTO a reduced permeation of T into the coolant as well as a facilitation of the tritium processing may be obtained. Despite the benefits, it must be taken into account that the addition of water vapor could alter the chemical form of solid/gas in the blanket. Kiat et al. reported the evolution of $\text{LiOH}(\text{s,l})$ at high temperatures, including the temperature shift of the phase transformation between $\text{Li}_2\text{O}(\text{s})$ and $\text{LiOH}(\text{s})$ depending on the H_2O concentration.^[7] This implies that a decomposition product of the ternary oxides could differ depending on the

humidity in the blanket. It was reported, by using Knudsen effusion mass spectrometry ($T > 1223$ K), that the addition of water enhanced the volatility of LiOH(g) from Li_4SiO_4 and Li_2TiO_3 , while Li(g) was a dominant Li-containing gas in dry D_2 gas condition.^{[8][9]} In fact, mass loss due to evaporation was reported to increase by addition of H_2O during heating at 1173 K.^[10] Such changes in phase equilibria of solid/gas might affect the corrosion behavior, however, chemical compatibility study between ceramic breeder and EUROFER steel has been limited to dry sweep gas atmosphere.^{[11][12]} In our previous work, the compatibility was also studied under the dry sweep gas condition, in which an unintended increase of H_2O concentration due to an interruption of the gas supply hinted at a formation of a thicker oxidized layer, suggesting a critical influence of moisture on the compatibility.^[13]

This study aims at examining the effect of water vapor on the chemical compatibility between ceramic breeder and EUROFER plate. These materials were kept contacted and heated for up to 3 month at 623, 823, and 1073 K under humid atmosphere. Then, these specimens were characterized by x-ray diffraction (XRD), scanning electron microscopy (SEM) combined with energy dispersive x-ray microanalysis (EDX), and secondary ion mass spectrometry (SIMS). The results were quantitatively analyzed based on diffusion kinetics for obtaining effective diffusion coefficient and then compared with the previous results in the dry sweep gas condition. The possible thickness of a corrosion layer on EUROFER plate after the use for 2 years was predicted by using the coefficient at 623 K.

Method

In figure 1, schematic image of the tube furnace and the alumina container is represented. A breeder pellet was sandwiched between two EUROFER 97 plates in the container by using a Inconel spring. Five of the alumina containers were heated at 623, 823, or 1073 K in T3 alumina tube (figure 1) and extracted after given times as follows. These five containers were extracted after 3, 7, 14, 21, and 28 days in the heating experiments at 823 and 1073 K, while those were taken after 7, 14, 28, 56, and 84 days in case of 623 K. During a sample extraction, temperature of the furnace was cooled down to 573 K. The CuO bed was heated at 723 K to supply water vapor into T3 tube as a result of the reduction of CuO particles to copper metal. N-type thermocouple was placed at the center of the heated zone in the furnace outside the alumina tube. Flow gas rate and pressure were controlled to be 1200 ml/min and 1.2 bar, respectively. The breeder pebbles with the two-phase composition (Li_4SiO_4 with 20 mol% of Li_2TiO_3), fabricated by the melt process,^[14] were crushed and then shaped into a pellet with a diameter of 8 mm. The breeder pellets were heated at 1123 K in Ar gas flow condition for 5 hours. The sintering density of the pellets was in the range of 90 to 92%.

After the heating experiments, XRD was carried out with a Bruker D8 using $\text{Cu-K}\alpha$ radiation by collecting diffraction data in the 2θ range from 15 to 70° . The polished surface of the EUROFER plate before the heating test exhibited a diffraction pattern of ferritic steel ($\alpha\text{-Fe}$) body-centered-cubic (bcc) structure. It is noted that the heating temperature of 1073 K is lower than the ferrite-austenite ($\alpha\text{-}\gamma$) transformation temperature of EUROFER97, which is reported to be 1099 K for an infinitely slow heating rate.^[15] XRD patterns were analyzed by Rietveld analysis by using TOPAS-academic software, by refining lattice parameter while fixing atomic position, occupancy, and isotropic displacement parameter because of weak intensity and high orientation. Cross-sections were studied by scanning electron microscopy (SEM SUPRA 55 by Zeiss) with an angle selective backscatter (AsB) detector to visualize a compositional contrast. Element distributions were investigated by energy dispersive X-ray microanalysis (EDX, Genesis XM2, Apollo 40 detector). For a SIMS measurement, the EUROFER plate heated at 1073 K for 3 days was chosen because a thick corrosion layer is unsuitable for the time-consuming sputtering process. The specimen was sputtered by oxygen primary ion using the ion source (IG-20 by Hiden) and then analysed by the quadrupole mass analyser (MAXIM by Hiden).

Though SIMS measurement originally gave information of element profile as a function of time, the time was converted into distance from surface x by measuring the depth of the ion eroded crater using the Bruker's DektakXT profilometer. Based on a constant sputtering rate during the measurement and by assuming it to be independent of any compositional changes, even in case of a corrosion layer, the rate of the EUROFER was estimated to be 0.20 ± 0.03 .

The effective diffusion coefficient of Li into EUROFER was estimated from the result of SIMS measurement by considering a simple case of diffusion to the bulk. In this case, count of the mass analyser C can be fitted by using the complementary error function as follows:

$$C = C_0 \operatorname{erfc}\left(\frac{x}{2\sqrt{Dt}}\right) \quad (1)$$

where C_0 , D , and t are count on the surface, diffusion coefficient (cm^2/s), and heating period (s), respectively.

In addition to the above approach, effective diffusivity of oxygen was estimated by measuring the thickness of the oxygen layer detected by SEM/EDX. The effective diffusion coefficient of oxygen D (cm^2/s) is given as follows:

$$D = d^2/t \quad (2)$$

where d is the thickness of the oxidized layer on the EUROFER plate and t is the heating period. The oxygen diffusion coefficient at each temperature was derived by plotting the square of d against t and then by fitting with a straight line from the origin.

Result and Discussion

Heating test

Figure 2 shows averaged moisture concentrations of the outlet gas, in which period 1 is the initial period until the first sample extraction and period n ($n > 1$) represents the heating period between $n-1^{\text{th}}$ and n^{th} extraction. The initial moisture concentrations were approximately 8 vol.% and decreased gradually to approximately 4 vol.%, while those in the tube with the dry sweep gas were in the range of 0.2 to 0.7 vol.%. The downward trend of moisture occurred mainly because the CuO particles became less capable of supplying H_2O with age due to a progression of the reduction. As mentioned in the previous paper,^[13] gas supply was interrupted after 25 days during the heating experiment at 823 K.^[13] Since the last alumina container was heated without gas supply for the remaining 3 days, the specimen heated at 823 K for 4 weeks was not evaluated in this paper.

Ceramic breeder

XRD patterns from the breeder pellets heated at 1073 K for the periods from 1 to 4 weeks are shown in figure 3. The diffraction after heating for 1 week remained to be the two-phase pattern of Li_4SiO_4 ($P2_1/m$) and Li_2TiO_3 ($2C/c$). In the patterns after heating for 2-4 weeks, the diffraction peaks from the Li_2SiO_3 phase ($2C/c$), which was not detected in the dry condition, were additionally found. The peak intensities of Li_2SiO_3 increased with heating period, while those of Li_4SiO_4 gradually weakened and shifted to lower 2θ (see inset). These changes indicated that Li_4SiO_4 phase gradually decomposes into Li_2SiO_3 . Figure 4 displays XRD patterns from the breeder pellets at 623 K for 12 weeks and at 823 K for 3 weeks. These patterns indicated that the surface of these specimens basically remained to be the two phase of Li_4SiO_4 and Li_2TiO_3 . In addition to these initial phases, traces of Li_2SiO_3 and Li_2CO_3 phase were detected. Li_2CO_3 may derive from a solid phase of Li_2O or

LiOH produced together with Li_2SiO_3 by the decomposition of Li_4SiO_4 . Since there should be a little amount of carbon in the inlet gas, Li_2CO_3 phase possibly formed from Li_2O or LiOH by exposure to air during a sample extraction and cooling down. Another possible source of carbon might be from the EUROFER specimen since carbon depletion from surface of JLF-1 ferritic-martensitic steel (Fe-9Cr-2W-0.1C) is reportedly caused by the immersion test in liquid Li with low concentration of carbon.^[16]

Figure 5 represents the change of cell volumes of the Li_4SiO_4 and the Li_2TiO_3 phase as a result of Rietveld refinements. It should be noted that the refinements resulted in poor fittings and high R factors ($R_{\text{wp}} = 19.6-24.2$, $R_p = 14.7-18.6$, and goodness-of-fit = 2.5-3.3), although all peaks were indexed by the two phases. Shrinkage of the Li_4SiO_4 cell volume was found in case of heating at 1073 K, which gradually decreased with heating period to $V/V_0 = 98.91(4)\%$ after 4 weeks. The shrinkage of Li_4SiO_4 at 1073 K progressed faster than that in the dry atmosphere, indicating the decomposition of Li_4SiO_4 was enhanced by addition of moisture. The cell volume of Li_4SiO_4 slightly decreased to $V/V_0 = 99.85(3)\%$ after 3 weeks in case of 823 K, while the shrinkage was not clearly seen at 623 K (data not shown). On the other hand, the cell volume of Li_2TiO_3 did not show a significant change, even after weeks of heating at 1073 K. This means that decomposition in the breeder material is preferably caused by the Li_4SiO_4 phase due to its lower thermodynamic stability.

To clarify solid products by decomposing reactions of Li_4SiO_4 in the breeder specimens, in figure 6, the moisture concentrations and the heating temperatures in the present and the previous work are plotted in the quasi-static phase diagram of $\text{LiOH-Li}_2\text{O}$ by Kiat.^[7] It is noted that the diagram was built by using $\text{LiOH}\cdot\text{H}_2\text{O}$ specimen and by performing thermogravimetry and differential scanning calorimeter experiments at the heating rate of 1 K/min up to 900 K with increasing partial pressure of H_2O . The moisture concentrations of the present experiment at 623, 823, and 1073 K in figure 2 were averaged to be 5.7 ± 0.5 , 7.5 ± 0.6 , and 6.5 ± 0.7 vol.% (52 ± 5 , 67 ± 6 , and 58 ± 6 mmHg in the phase diagram). As seen in figure 6, 823 and 1073 K in the wet conditions as well as all the temperatures in the dry condition were positioned above the transformation temperature of the solid-solid phase transformation between LiOH(s) and $\text{Li}_2\text{O(s)}$. In such cases, Li_4SiO_4 decomposes into solid phases of Li_2O and Li_2SiO_3 as follows.



On the other hand, 623 K in the wet condition was below the temperature of the phase transformation. In this environmental condition, Li_4SiO_4 decomposes into solid phases of Li_2SiO_3 and LiOH by reacting with water vapor.



The difference in the produced solids could have an influence on corrosion of EUROFER steel since Li_2O and LiOH are known to be more chemically reactive at high temperature compared with the ternary oxides.

Based on the phase diagram, it should be noted that an addition of moisture to the sweep gas would allow a portion of bred tritium to form the solid phase of LiOT , which might result in an increase of tritium inventory in the blanket.

EUROFER

Figure 7 displays SEM image and EDX mappings of the cross section of the EUROFER plate heated at 1073 K for 3 days. The SEM image clearly shows formation of the double oxide layer on the surface of the EUROFER plate as found in the dry condition.^[13] EDX mappings indicated that the outer and the inner layer

had a high concentration of Fe and Cr, respectively. The thickness of the corrosion layer, namely the sum length of the outer and the inner layer, was $21 \pm 5 \mu\text{m}$. Similar characteristics can be seen in depth profiles by SIMS on the same EUROFER plate (3 days, 1073K) as shown in figure 8. The Cr signal was significantly reduced in the outer layer ($x < 8 \mu\text{m}$), whereas a rich abundance of Cr was seen in the inner layer ($8 < x < 20 \mu\text{m}$). The Li content was almost constant in these oxidized layers and showed a moderate drop at $x > 18 \mu\text{m}$. Since the Li drop seem to be linked to the abundance of O and Cr rather than that of Fe, Li diffusion into chromium oxide might have occurred to form Li-Cr-O compounds such as LiCrO_2 . The Li drop was fitted by the error function of eq. (1) as represented by the orange line shown in the inset of figure 8. The fitting curve yielded diffusion coefficient of Li into EUROFER to be $9.2 \times 10^{-14} \text{ cm}^2/\text{s}$. The coefficient was faster than that in the dry atmosphere at 1073 K ($1.3 \times 10^{-14} \text{ cm}^2/\text{s}$), indicating an enhancement of Li diffusion by moisture. The elevation of the Si content near the interface between the inner oxide layer and the α -Fe bulk should be corresponding to a Si segregation as found in the previous paper.^[13] Figure 9 shows the SEM image and EDX mappings of the cross section of the EUROFER plate heated for 12 weeks at 623 K. The EDX mappings showed that the scale was mainly composed by outer Fe-rich oxide layer, while inner Cr-rich oxide layer was very thin. Like in the dry condition, XRD from the surface of the specimen (data not shown) indicated the formation of LiFe_5O_8 and Fe_2O_3 phases as well as the remaining α -Fe phase.

Evolutions of the corrosion layers with heating period were found at all the temperatures. The thickness of the double oxide layer on the EUROFER after 4 weeks was approximately $30 \mu\text{m}$, which was much smaller than that of 3 weeks ($158 \pm 15 \mu\text{m}$). This EUROFER specimen possibly underwent a peel-off after a growth of a thick corrosion layer and then a reformation of the double oxidized layer. As expected, the formation of the oxidized layer was significantly enhanced by moisture when heating at 823 and 1073 K. For example, the thicknesses on the EUROFER plates heated in the wet condition for 3 weeks at 823 and 1073 K were 46.5 ± 2.6 and $158 \pm 15 \mu\text{m}$, respectively, while those in the dry condition were 7.4 ± 0.9 and $26.3 \pm 1.6 \mu\text{m}$. However, the influence was limited in the experiment of 623 K: the thickness after 12 weeks at 623 K was $5.9 \pm 1.0 \mu\text{m}$ (figure 9), compared to that in the dry gas condition with $3.5 \pm 0.1 \mu\text{m}$. The smaller impact of moisture at 623 K may result from the fact that an evaporating reaction from LiOH (e.g. $2\text{LiOH}(\text{s}) \leftrightarrow 2\text{Li}(\text{g}) + 0.5\text{O}_2(\text{g}) + \text{H}_2\text{O}(\text{g})$) was suppressed by the high concentration of water vapor.

In figure 10, the square of the oxidized layer thicknesses are plotted. Due to its fragility, the corrosion layer was broken during preparations and therefore some data points are missing in the graphs. The data at 1073 K after 4 weeks was eliminated because of the reformation of the double oxidized layer. The plots were fitted by straight lines from the origin based on eq. (2). The fittings in the present work were not so good as in the dry condition, especially at 1073 K, due to harsh surfaces as a result of intensive corrosion. The straight fitting lines at 623, 823, and 1073 K yielded effective oxygen diffusion coefficients as of $D = 4.5 \times 10^{-13}$, 1.1×10^{-10} , and $1.3 \times 10^{-9} \text{ cm}^2/\text{s}$, which were faster than that of Li at 1073 K. The given coefficients at 823 and 1073 K were approximately one order of magnitude faster than those in the dry condition, whereas the ones at 623 K in both atmospheres were in the same order. In figure 11, the given diffusion coefficients in this work (wet) as well as the previous work (dry) are plotted in an Arrhenius plot. As the coefficients in the wet condition cannot be approximated by a single straight line, instead a line (blue dot in figure 10) was made by the two data points at the elevated temperatures while ignoring the data at 623 K. Based on Arrhenius equation, the slope of the line yielded an activation energy of 1.01 eV. The given energy seems reasonable because it is in good agreement with the one given in the dry condition (0.93 eV) and the previous study for oxygen diffusion into bcc α -Fe alloy (0.89-1.03 eV).^{[17]-[19]} At 623 K, an order of magnitude discrepancy was found between the given diffusion coefficient and an extrapolated one from the line. This emphasizes that an extrapolation from data of elevated temperatures is not feasible in the

wet condition, while compatibility tests have often been carried out by heating at an elevated temperature, such as 823 or 873 K, as an accelerated condition.^{[1][12]}

By a temporal extrapolation using the effective diffusion coefficient of oxygen at 623 K, a thickness of the corrosion layer on EUROFER structural steel contacted with the breeder pebble after an operation period can be predicted. Given the ceramic breeder pebble is packed in the blanket of EUROFER steel and used for 2 years at 623 K, the length of corrosion layer would be 53 μm , compared with 32 μm in the dry sweep gas. This level of corrosion caused by contacted breeder pebbles would have a limited influence on the strength of the structural steel because it corresponds to approximately 4% of the minimum thickness (1.25 mm) of the structural steel in the HCPB blanket.^[1] Yet, further assessment is necessary for applying moisture in sweep gas since the Li-containing gas species evaporated in a high temperature region of the pebble bed might be transported by the sweep gas to an outlet pipe of the blanket and then form a corrosion layer.

Conclusion

In this study the influence of moisture in sweep gas on the chemical compatibility between ceramic breeder and EUROFER97 was investigated by heating them at 623, 823, and 1073 K in moisture concentrations of 4-8 vol.%. In the breeder specimens heated at 1073 K, a gradual formation of Li_2SiO_3 phase on the surface was found as a result of decomposition of Li_4SiO_4 , which was not seen in the dry atmosphere. Traces of products resulting from the decomposition were also found at 623 and 823 K. Accordingly, formation of the double oxide layer on EUROFER was critically enhanced by the moisture addition, especially in elevated temperatures of 823 and 1073 K. But, the effect of moisture was limited in case of heating at 623 K, which can be attributed to different chemical form in the breeder specimens, namely Li_2O or LiOH . The effective diffusion coefficient of oxygen into EUROFER at 673 K was given to be $D = 4.5 \times 10^{-13} \text{ cm}^2/\text{s}$ and faster than that of Li diffusion at 1073 K. Thickness of corrosion layer on EUROFER structural steel after use of 2 years was estimated to be 53 μm , which should be still acceptable level compared with the minimum thickness of the blanket. Yet, for employing wet sweep gas, further researches should be carried out on tritium recovery and an indirect corrosion caused by evaporated gas species.

Acknowledgement

This work has been carried out within the framework of the EUROfusion Consortium and has received funding from the Euratom research and training programme 2014-2018 under grant agreement No 633053. The views and opinions expressed herein do not necessarily reflect those of the European Commission.

Reference

- [1] F. Hernández, P. Pereslavytsev, Q. Kang, P. Norajitra, B. Kiss, G. Nadási, O. Bitz, under review for Nuclear Materials and Energy as proceedings of the SOFT 2016 in Prague.
- [2] D.L. Smith, M.C. Billone, S. Majumdar, R.F. Mattas, D.K. Sze, J. Nucl. Mater., 258, 1998, 65-73.
- [3] R. Lindau, A. Möslang, M. Rieth, M. Klimiankou, E. Materna-Morris, A. Alamo, A.-A. F. Tavassoli, C. Cayron, A.-M. Lancha, P. Fernandez, N. Baluc, R. Schäubline, E. Diegele, G. Filacchioni, J.W. Rensman, B.v.d. Schaaf, E. Lucon, W. Dietz, Fusion Eng. Des. 75 (2005) 989-996.
- [4] R. Knitter, M. H. H. Kolb, U. Kaufmann, A.A. Goraieb, J. Nucl. Mater. 442 (2013) S433-S436.
- [5] K. Munakata, T. Shinozaki, K. Inoue, S. Kajii, Y. Shinozaki, R. Knitter, N. Bekris, T. Fujii, H. Yamana, K. Okuno, Fusion Eng. Des. 83 (2008) 1317-1320.

- [6] M. Nishikawa, T. Kinjyo, T. Ishizaka, S. Beloglazov, T. Takeishi, M. Enoeda, and T. Tanifuji, *J. Nucl. Mater.* 335(1) (2004) 70-76.
- [7] J.M. Kiat, G. Boemare, B. Rieu, D. Aymes, *Sol. St. Comm.* 108 (1998) 241-245.
- [8] M. Yamawaki, A. Suzuki, M. Yasumoto, K. Yamaguchi, *J. Nucl. Mater.* 247 (1997) 11-16.
- [9] A. Suzuki, M. Yamawaki, M. Yasumoto, K. Yamaguchi, *J. Nucl. Mater.* 248 (1997) 111-115.
- [10] K. Katayama, H. Kashimura, T. Hoshino, M. Nishikawa, H. Yamasaki, S. Ishikawa, Y. Ohnishi, S. Fukada, *Fusion Eng. Des.* 87 (2012) 927-931.
- [11] L.C. Alves, E. Alves, M.R. da Silva, A. Paúl, A. La Barbera, *J. Nucl. Mater.* 329 (2004) 1295-1299.
- [12] T. Hernández, P. Fernández, R. Vila, *J. Nucl. Mater.* 447 (2014) 160-165.
- [13] K. Mukai, F. Sanchez, R. Knitter, “Chemical compatibility study between ceramic breeder and EUROFER97 steel for HCPB-DEMO blanket”, under review for *J. Nucl. Mater.*
- [14] M. H. Kolb, R. Knitter, U. Kaufmann, D. Mundt, *Fusion Eng. Des.* 86 (2011) 2148-2151.
- [15] K.D. Zilnyk, V.B. Oliveira, H.R.Z. Sandim, A. Möslang, D. Raabe, *J. Nucl. Mater.* 462 (2015) 360-367.
- [16] Q. Xu, M. Kondo, T. Nagasaka, T. Muroga, O. Yeliseyeva, *J. Nucl. Mater.* 394 (2009) 20-25.
- [17] J. Takada, M. Adachi, *J. Mater. Sci.* 21 (1986) 2133-2137.
- [18] J.H. Swisher, E.T. Turkdogan, *Trans. Met. Soc. AIME* 239 (1967) 426-431.
- [19] W. Frank, H.J. Engell, A. Seeger, *Z. Metallkd.* 58 (1967) 452-455.

Figures

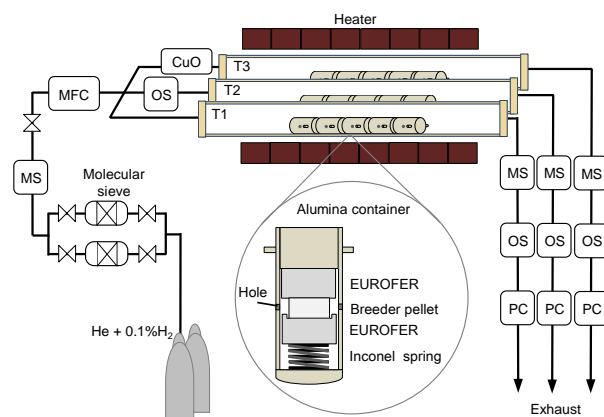


Figure1 Schematic image of the alumina container and the tube furnace connected with moisture sensor (MS), mass flow controller (MFC), oxygen sensor (OS), and pressure controller (PC). Five of the alumina containers were heated in the tube T3 connected with copper oxide (CuO) bed.

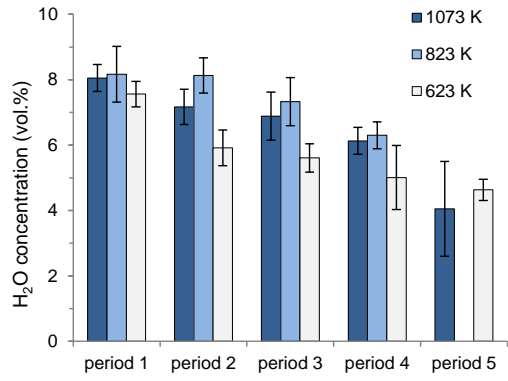


Figure2 Moisture concentrations of the outlet gas in each heating period.

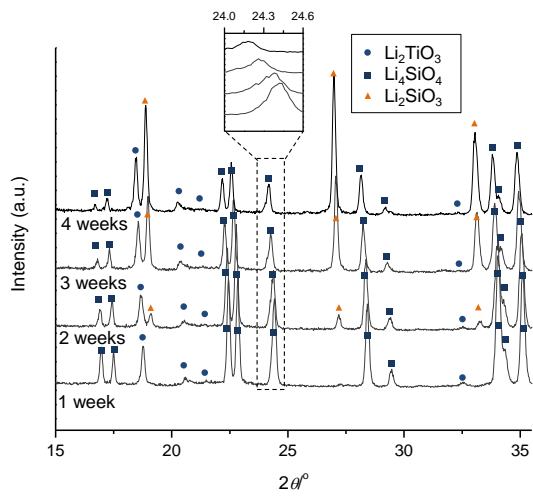


Figure3 XRD patterns from the breeder pellets heated at 1073 K for the periods from 1 to 4 weeks.

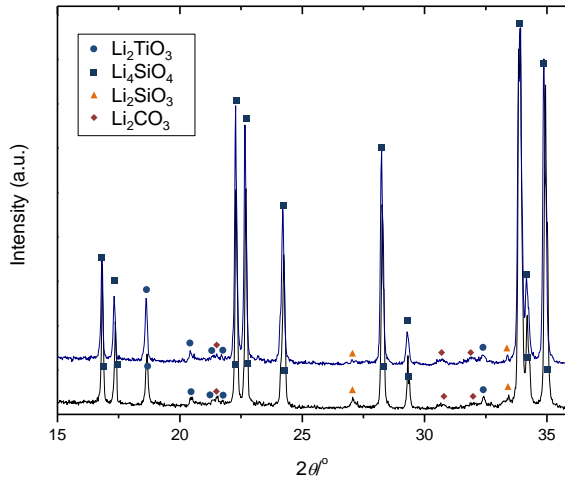


Figure 4 XRD patterns from the breeder pellets heated at 623 K for 12 weeks (lower black) and 823 K for 3 weeks (upper blue).

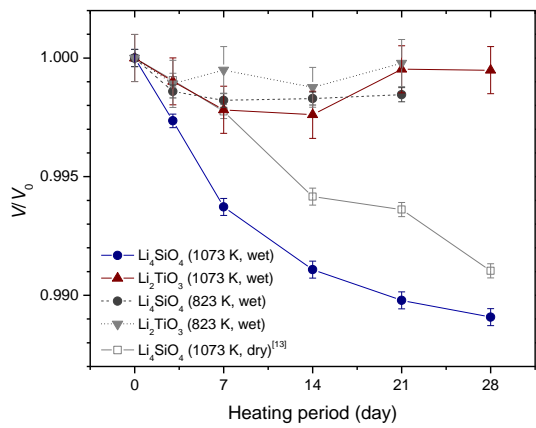


Figure 5 Changes in the cell volumes of the Li₄SiO₄ and the Li₂TiO₃ phase with heating period obtained by the Rietveld analysis using XRD data from the breeder pellet heated at 1073 K in the humid and the dry atmosphere,^[13] in which V_0 denotes the initial cell volume before the compatibility test.

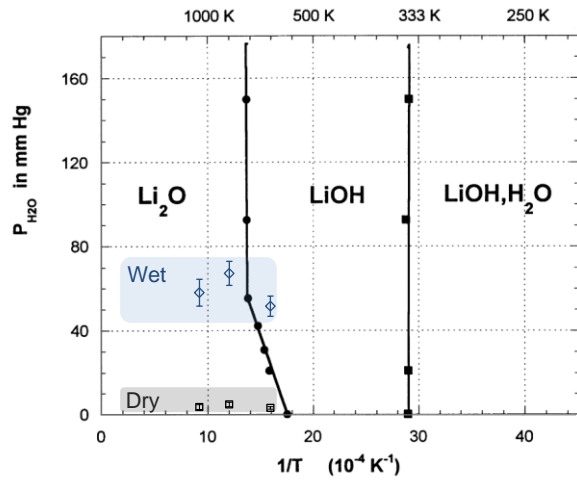


Figure 6 Temperature and partial pressure of water in this work (wet) and the previous work (dry), plotted in the phase diagram of Li_2O - LiOH system by Kiat et al.^[7]

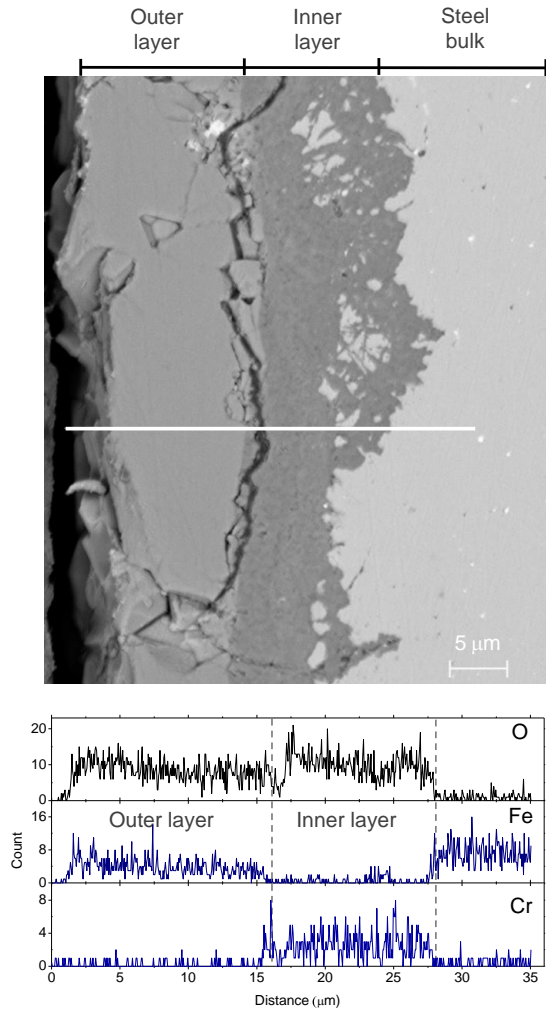


Figure 7 SEM image and EDX line scan on the cross section of the EUROFER plate heated at 1073 K for 3 days.

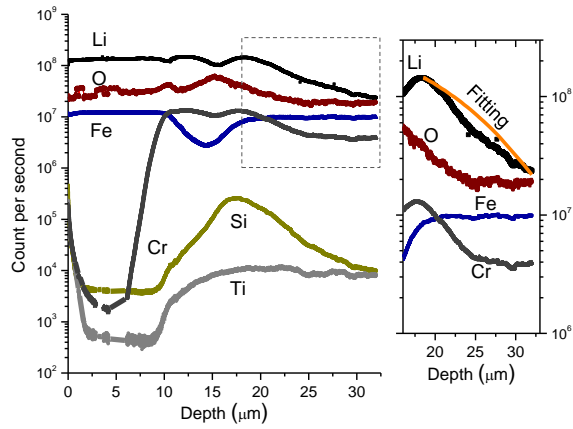


Figure 8 SIMS depth profiles of the EUROFER plate heated at 1073 K for 3 days.

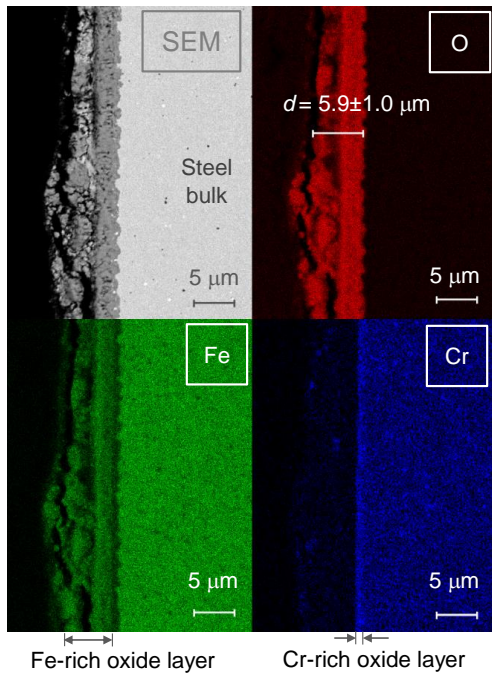


Figure 9 SEM image and EDX mappings of the cross section of the EUROFER plate heated at 623 K for 12 weeks.

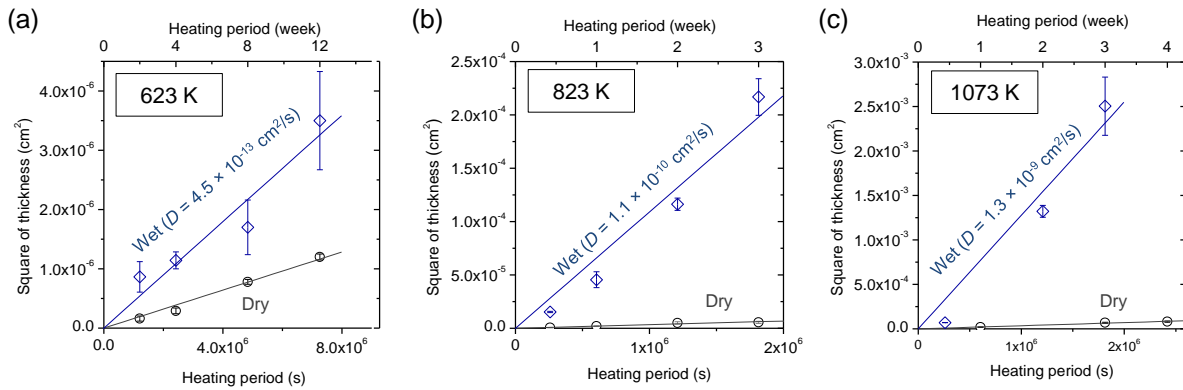


Figure 10 Square of oxidized layer thickness on the surfaces of the EUROFER plates heated at 623 (a), 823 (b), and 1073 K (c) in the wet and the dry condition with straight fitting lines from the origin resulting in the given effective oxygen diffusion coefficients D .

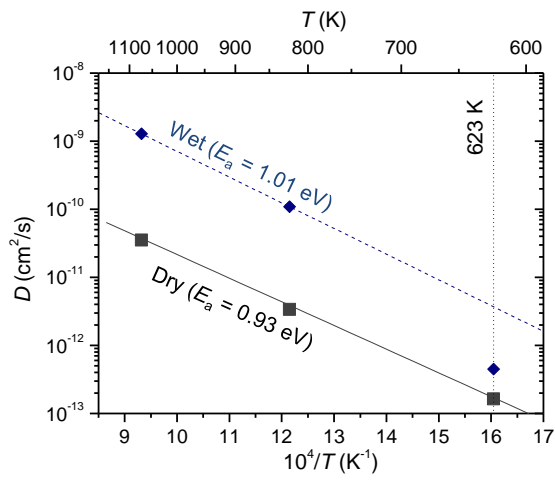


Figure 11 Arrhenius plot of effective oxygen diffusion coefficient obtained in the present (wet) and the previous work (dry).^[13]